User Calibration-free Method using Corneal Surface Image for Eye Tracking

Sara Suda[1], Kenta Yamagishi[2] and Kentaro Takemura[1,2]
[1]*Graduate School of Engineering, Tokai University, Hiratsuka, Japan*
[2]*Department of Applied Computer Engineering, Tokai University, Hiratsuka, Japan*

Keywords: User Calibration-free, Corneal Surface Image, 3D Eye Model.

Abstract: Various calibration methods to determine the point-of-regard have been proposed for eye tracking. Although user calibration can be performed for experiments carried out in the laboratory, it is unsuitable when applying an eye-tracker in user interfaces and in public displays. Therefore, we propose a novel calibration-free approach for users that is based on the use of the corneal surface image. As the environmental information is reflected on the corneal surface, we extracted the unwarped image around the point-of-regard from the cornea. The point-of-regard is estimated on the screen by using the unwarped image, and the regression formula is solved using these points without user calibration. We implemented the framework of the algorithm, and we confirmed the feasibility of the proposed method through experiments.

1 INTRODUCTION

In recent years, eye-tracking technology has improved to a remarkable extent; thus, the future use of an eye-tracker for applications such as marketing and user interfaces can be expected. Various approaches have been proposed for estimating the point-of-regard, and the eye-tracking method can roughly be classified into two types. The conventional method involves an approach based on regression, in which the point-of-regard is calculated using the Purkinje point and the center of the pupil. In contrast, the visual axis is calculated for estimating the point-of-regard when we employ the model-based approach. Both of these methods require user calibration to be performed before determining the point-of-regard, but the calibration is a cumbersome process for the user.

Therefore, calibration-free methods have been studied actively. Nagamatsu et al.(Nagamatsu et al., 2009) developed a user calibration-free method for calculating the two visual axes using the optical axes of both eyes. The point-of-regard is estimated using the two visual axes on the display plane, and high accuracy was achieved. However, it needs the location of display and camera as hardware calibration. Additionally, Sugano et al.(Sugano and Bulling, 2015) proposed user calibration-free gaze tracking using a saliency map, whereby calibration is achieved automatically when the user looks at the scene for a while. In fully automatic calibration, gaze can be estimated around 10 degrees without user-calibration and hardware calibration. Khamis et al.(Khamis et al., 2016) proposed an implicit calibration that correlates users' eye movements with moving on-screen targets while the user is simply reading this text. We also started to study a calibration-free method for users based on this background, but our motivation is to achieve the calibration without the geometrical restriction, and the point-of-regard is estimated immediately. Our aim is to solve these problems by focusing on the corneal-imaging technique(Nishino and Nayar, 2006). This technique acquires the environmental information from the reflection of the surface of the cornea. Nitschke et al.(Nitschke and Nakazawa, 2012) proposed to obtain a high-resolution image by super-resolution, and Wang et al.(Wang et al., 2005) succeeded in removing the texture of the iris from the image. Additionally, Takemura et al.(Takemura et al., 2014) the method for estimating the focused object using corneal-imaging technique. Therefore, we expect the corneal-imaging technique to be a breakthrough for solving the calibration problem, and we propose a calibration-free method for users for eye tracking using the corneal surface image.

The remainder of this paper is organized as follows. First, the 3D eye model is introduced in section 2, after which model-based iris tracking is described in section 3. Then, a method for generating the un-

Suda S., Yamagishi K. and Takemura K.
User Calibration-free Method using Corneal Surface Image for Eye Tracking.
DOI: 10.5220/0006100100670073
In *Proceedings of the 12th International Joint Conference on Computer Vision, Imaging and Computer Graphics Theory and Applications (VISIGRAPP 2017)*, pages 67-73
ISBN: 978-989-758-227-1

warped image from the corneal surface image is explained in section 4. A method that is calibration-free for users is proposed, and we confirm the feasibility of the method in section 5 and 6, respectively. Finally, section 7 presents our conclusions and our future work.

2 GENERATING THE 3D EYE MODEL

A 3D model of the eye is used for tracking the iris and extracting the corneal surface image. This model consists of the corneal sphere and the eyeball as shown in Figure 1, and four anatomical parameters are defined as in Table 1. The position of the 3D eye is determined by the size of the iris; therefore, the area of the iris is detected using an elliptical approximation as shown in Figure 2. The radii of the major and minor axes of the iris area are r_{max} and r_{min}, respectively, and (i_{Lx}, i_{Ly}) is the center of the iris. When the edges of the iris area are selected as the initial stage, the 3D eye model is generated by the following equations. The distance d from the image plane to the 3D limbus center is defined by

$$d = f\frac{r_L}{r_{max}}, \tag{1}$$

and the 3D limbus center $\mathbf{L}$ is determined by the following equation:

$$\mathbf{L} = \left[d\frac{i_{Lx}-cx}{f}, d\frac{i_{Ly}-cy}{f}, d\right]^T, \tag{2}$$

where (cx, cy) and f are the center of the image and the focal length, respectively. The 3D limbus is the intersection of the eyeball and the corneal sphere, and it is the border of the iris. The optical vector $\mathbf{g}$ is estimated based on the 3D limbus center by the following equation:

$$\mathbf{g} = [\sin(\tau)\sin(\phi), -\sin(\tau)\cos(\phi), -\cos(\tau)]^T, \tag{3}$$

where ϕ is the rotation of the limbus ellipse, and τ is the tilt of the iris on the 3D eye model and is computed by

$$\tau = \pm cos^{-1}\left(\frac{r_{min}}{r_{max}}\right). \tag{4}$$

The center of the corneal sphere $\mathbf{C}$ and the center of the eyeball $\mathbf{E}$ are defined by the two following equations, respectively:

$$\mathbf{C} = -d_{LC}\frac{\mathbf{g}}{\|\mathbf{g}\|} + \mathbf{L}, \tag{5}$$

$$\mathbf{E} = -(r_{LE} - r_C)\frac{\mathbf{g}}{\|\mathbf{g}\|} + \mathbf{C}. \tag{6}$$

Finally, the position of the 3D eye model is computed as shown in Figure 3.

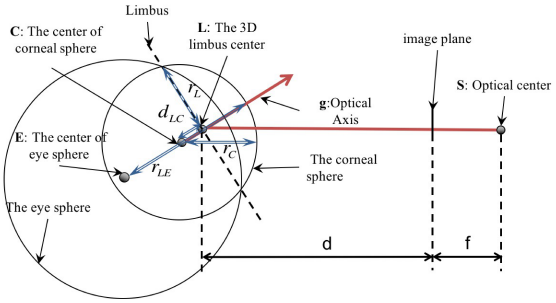

Figure 1: Geometric 3D eye model consisting of the eye sphere and the corneal sphere.

Table 1: Parameters of the eyeball model as defined by anatomical data.

Eyeball parameters	Size[mm]
Radius of corneal sphere(r_C)	7.78
Distance between corneal surface and eyeball center(r_{LE})	13.00
Distance between center of corneal sphere and center of iris (d_{LC})	5.60
The radius of the iris (r_L)	5.60

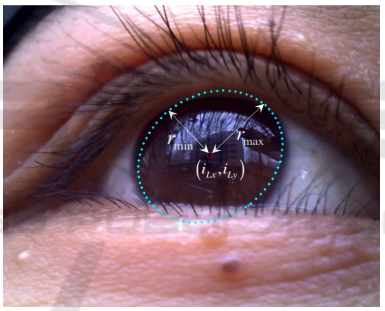

Figure 2: Area of the iris estimated using an elliptical approximation.

3 MODEL-BASED IRIS TRACKING

We employed an RGB camera for extracting the reflection of the cornea. Therefore, the iris is the tracking object, and its area has to be detected continuously. As mentioned above, the position of the 3D eye model is computed; thus, the iris can be tracked using the 3D eye model. The rotation center is equal to the center of the eyeball generally, so we also assumed that the generated eye model is rotated on the center of eyeball by the yaw and pitch angle for detecting the current pose. Our algorithm compares the binary image $\mathbf{B}$ and the projected iris areas $\mathbf{I}$ from the rotated 3D model as shown in Figure 4, and the cur-

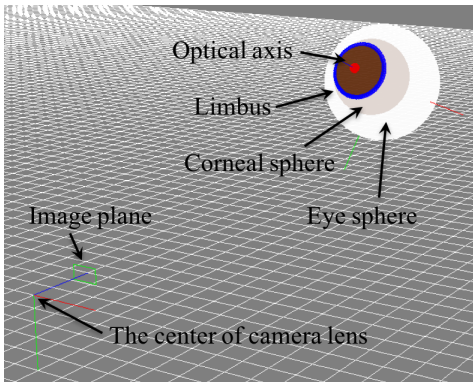

Figure 3: Generated 3D eye model consisting of the corneal sphere and the eye sphere.

rent pose is estimated by the following evaluation function:

$$\{\hat{\theta},\hat{\psi}\} = \arg\max_{\theta,\psi} \sum_{j=1}^{m}\sum_{i=1}^{n} \mathbf{B}_{ij}\mathbf{I}_{\theta\psi ij}, \tag{7}$$

where i and j are the image coordinates, and m and n are the size of the image. The maximum value is searched by using the hill-climbing algorithm, and we obtain the current pose as $\hat{\theta}$ and $\hat{\psi}$. However, the estimated area of the iris is influenced by the area covered by the eyelid area as shown Figure 5(a). As the objective of this research is to confirm the feasibility of a user calibration-free technique, we require a good tracking result for consideration. Therefore, we adjusted the estimated pose manually as shown in Figure 5(b).

4 GENERATING THE UNWARPED CORNEAL SURFACE IMAGE

The reflection image is distorted on the surface of the cornea; hence, the unwarped image is generated for estimating the point-of-regard. We assumed the reflection on the cornea to be a specular reflection, which is computed using the geometric relationship between the eye model and the input image as shown in Figure 6. The point **P** is the intersection of the corneal sphere and the optical axis of the eye, and the center of the tangent plane is located on **P**. When the point on the tangent plane and the center of camera lens are defined as **T** and **S**, respectively, the normal vector **N** is computed by the following equation:

$$\mathbf{N} = x\mathbf{S} + y\mathbf{T}, \tag{8}$$

where x and y satisfy the following equations under

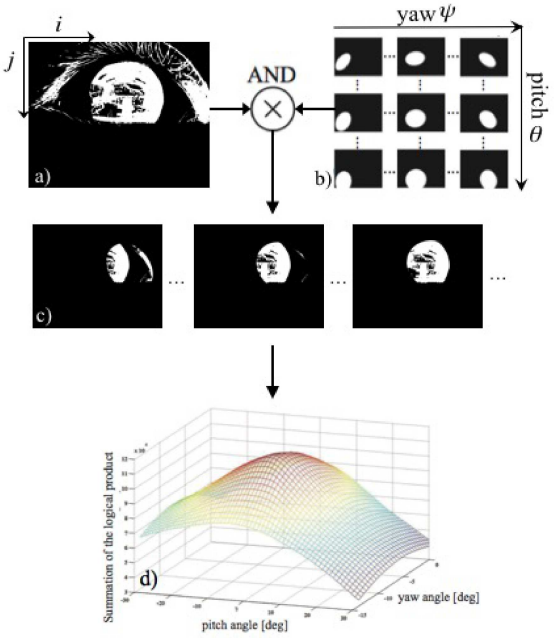

Figure 4: Algorithm for iris tracking using the 3D eye model. An inverted binary image(a) and the simulated images of the iris area (b) are used to compute the logical product of these images(c). In addition, the area of the iris is detected when the maximum value is found in the summed values of the logical product(d).

the constraint of the specular reflection:

$$\begin{aligned} 4cdy^4 - 4dy^3 + (a+2b+c-4ac)y^2 \\ +2(a-b)y + a - 1 = 0, \end{aligned} \tag{9}$$

$$x = \frac{(-2y^2+y+1)}{(2by+1)}, \tag{10}$$

where $a = \mathbf{S}\cdot\mathbf{S}$, $b = \mathbf{S}\cdot\mathbf{T}$, $c = \mathbf{T}\cdot\mathbf{T}$, $d = |\mathbf{S}\times\mathbf{T}|^2$ are defined. When the biquadratic equation Equation 9 is solved under the constraint $x > 0$ and $y > 0$, and the vector **N** is computed. The reflection point **R** on the surface of the corneal sphere is calculated by

$$\mathbf{R} = r_C \frac{\mathbf{N}}{\|\mathbf{N}\|}. \tag{11}$$

The unwarped image is created by the color information obtained from the point **R** on the corneal surface image. Actually, the color is extracted from the input image using inverse ray tracking for estimating the color of point **R**. For example, the unwarped image is generated as shown in Figure 7, and the edge of the basket is undistorted on the unwarped image.

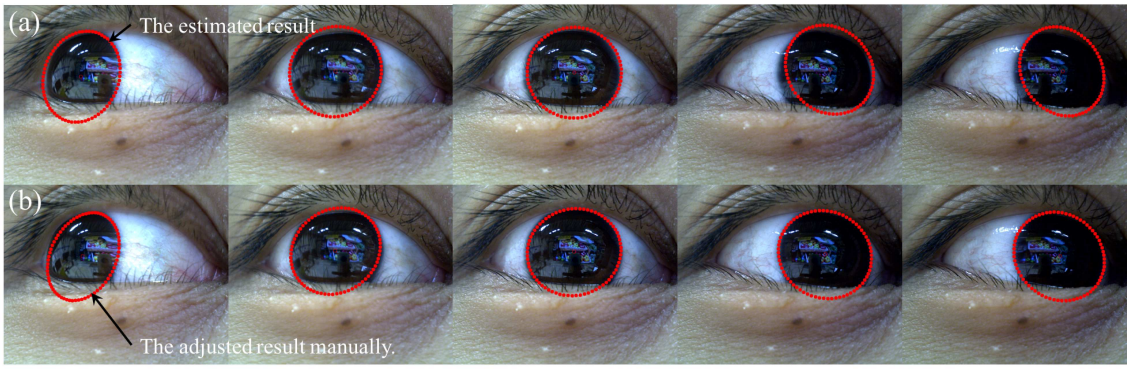

Figure 5: Area of the iris (a) estimated using model-based tracking, and (b) adjusted manually.

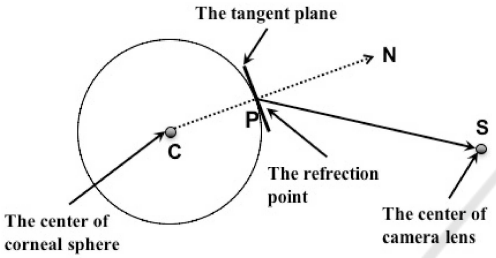

Figure 6: Relationship between the eye model and reflection point.

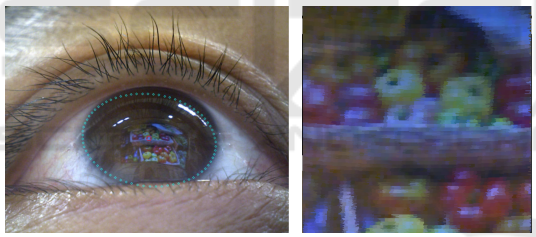

(a) input image (b) unwarped image

Figure 7: Image of the cornea (a) input image, and (b) generated unwarped corneal surface image.

5 USER CALIBRATION-FREE BASED ON CORNEAL SURFACE IMAGE

In general, a user would have to look at several points on a display for user calibration, because the visual axis of the eye and the relationship between the eye and the screen are determined to achieve high accuracy. In contrast, various methods have been proposed as being user calibration-free, but there are various constraints. In the case of using a model-based approach, the geometrical relationship between the camera and the display is known in advance. In the case of using regression-based approach, the user is required to look at the display for a while, which is why the point-of-regard cannot be estimated immediately. Therefore, we propose a user calibration-free method without these constraints by using the corneal surface image for providing high versatility.

5.1 Finding the Corresponding Area between the Unwarped Corneal Surface Image and the Display Image

In our method, it is necessary to search the corresponding area between the unwarped image and the display image. When the corresponding point is decided, the point is employed as the point-of-regard. Additionally, it is possible to collect the points and the eye pose for solving the regression formula. However, the scales of the unwarped image and the display image are different; thus, the scale is adjusted manually. When we select two matched points $E_{1,2}$ and $D_{1,2}$ on the unwarped image and the display image, respectively, then the scale $\mathbf{s}$ is calculated by the following equations:

$$[s_x, s_y] = \left[\frac{|D_{1x} - D_{2x}|}{|E_{1x} - E_{2x}|}, \frac{|D_{1y} - D_{2y}|}{|E_{1y} - E_{2y}|} \right]. \quad (12)$$

The scale of the unwarped image is adjusted using $\mathbf{s}$, and the reflection point is searched on the display image by template matching based on normalized cross correlation. The image of the reflection area is huge for detecting the corresponding area; thus, we extracted the image around the center of the unwarped image as the template image. Figure 8(a) shows the result of template matching when Figure 8(b) is employed as the template image.

The estimated corresponding area is the point-of-regard; thus, we can estimate the point-of-regard immediately. However, as the reflection on the cornea is influenced by the illumination condition, it is difficult to use the corresponding area continuously. Therefore, the regression formula is obtained for improving

Figure 8: Result image of template matching (a), and template image(b). The area within the square is the result of template matching.

the robustness. Details of the regression formula are described below.

5.2 Regression Formula Obtained using the Collected Point-of-regard

In the general regression approach, the Purkinje points and the pupil centers are collected to solve the regression expression when a user looks at several points. In contrast, in our approach the regression formula is solved while the point-of-regard is estimated using the unwarped image. After that, the point-of-regard is estimated by the regression expression using the pose of the eye.

The area of the display was divided into nine areas, and the regression expression was calculated by the nine points with a high cross-correlation value in each area. The poses of the 3D eye model are defined as $(\hat{\theta}_{1\ldots9}, \hat{\psi}_{1\ldots9})$, and the point-of-regard on the display image is also defined as $(u_{1\ldots9}, v_{1\ldots9})$. The regression formula is calculated by the following equation:

$$\begin{bmatrix} u_1, \cdots, u_9 \\ v_1, \cdots, v_9 \end{bmatrix} = \mathbf{A} \begin{bmatrix} \hat{\theta}_1, \cdots, \hat{\theta}_9 \\ \hat{\psi}_1, \cdots, \hat{\psi}_9 \\ 1, \cdots, 1 \end{bmatrix}. \quad (13)$$

The matrix of the coordinate values of the display image are defined as $\mathbf{M}$, and the parameters of the regression expression $\mathbf{A}$ is calculated using the pseudo-inverse matrix $\mathbf{M}^+$ by the following equation:

$$\mathbf{A} = \begin{bmatrix} \hat{\theta}_1, \cdots, \hat{\theta}_9 \\ \hat{\psi}_1, \cdots, \hat{\psi}_9 \\ 1, \cdots, 1 \end{bmatrix} \mathbf{M}^+. \quad (14)$$

Finally, the regression formula is obtained without the user calibration procedure, and when the current eye pose $(\hat{\theta}_c, \hat{\psi}_c)$ is determined, the point-of-regard **PoR** can also be estimated using the regression expression by the following equation:

$$\mathbf{PoR} = \mathbf{A} \begin{bmatrix} \hat{\theta}_c \\ \hat{\psi}_c \\ 1 \end{bmatrix}. \quad (15)$$

Figure 9: Environmental setup for the user calibration-free method.

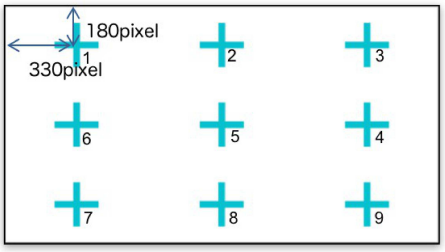

Figure 10: Image used for evaluating the accuracy of the estimated point-of-regard in the evaluation experiment.

6 COMPARATIVE EXPERIMENTS BETWEEN THE CONVENTIONAL CALIBRATION AND THE USER CALIBRATION-FREE METHOD

6.1 Experimental Condition

We performed comparative experiments between the conventional calibration and the user calibration-free method to evaluate the accuracy of the estimated point-of-regard. The four trial subjects wore the instrumental device consisting of the eye camera, and the subjects looked in every hole and corner of the display on which a still image is shown. Figure 9 shows the experimental condition, and the distance between the display screen and the trial subjects is 800 mm. In this experiment, it is not possible to use the chin rest as an experimental installation, but we requested subjects not to move their head.

6.2 Experimental Results

We solved the two regression formulas of the user calibration-free and the conventional methods, respectively. In the case of the conventional method, the calibration points, which are used for solving the regression expression, are collected manually. After solving two regression expressions, trail subjects

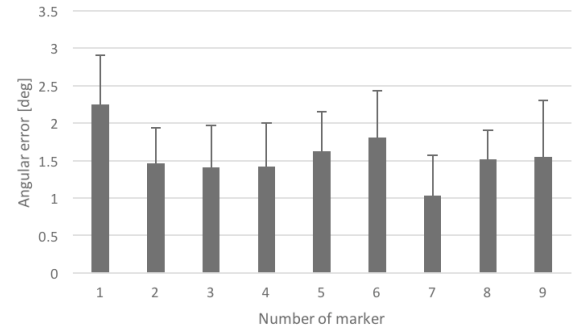

Figure 11: Angular error of the estimated PoR by the conventional method.

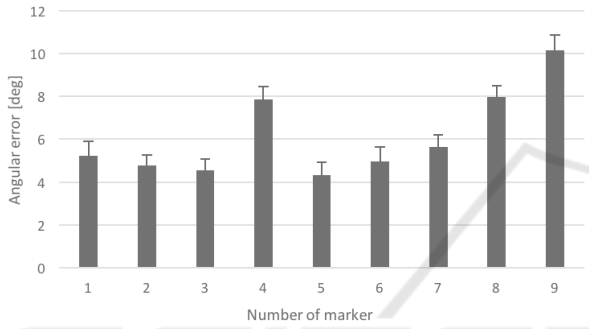

Figure 12: Angular error of the estimated PoR by the user calibration-free method.

were requested to look at an image on which nine crosses are drawn (Figure 10) for evaluating the estimated the point-of-regard. The angular errors of the conventional method and the proposed method were computed as shown in Figure 11 and Figure 12, respectively.

6.3 Consideration

Currently, the accuracy of the conventional method exceeds that of the proposed method; thus, we considered the cause of error through the results. In the case of using the conventional calibration method, the average of the angular error is 1.56 degrees, and the angular error of each marker is closed. On the other hand, the average of the angular error is 6.15 degrees in the case of using the proposed method, and there is great variability among each marker. We understood that the cause of difference depended on the performance of template matching, and it is necessary to improve the performance of extracting the image from the corneal surface.

7 CONCLUSIONS

In this paper, we proposed the user calibration-free technique based on the use of a corneal surface image. The corneal surface image was extracted using a 3D model of the eye, and the point-of-regard for solving the regression formula is estimated by template matching. We succeeded in solving the relationship between the display image and the eye pose using the regression expression, and we confirmed the feasibility of the framework for the user calibration-free based on the corneal surface image. The average of the angular error is around six degreesand the modest performance was achieved without user-calibration and hardware calibration. However, we identified the need for some improvements through the experiments. Currently, the accuracy is insufficient for using the point-of-regard in various applications; thus, the matching performance would have to be improved in future. Additionally, the operator is required to implement some manual settings; thus, it is difficult to achieve auto-calibration in the current implementation. These problems would need to be addressed to automate the calibration.

ACKNOWLEDGMENT

This work was supported by Grant Number 16H02860.

REFERENCES

Khamis, M., Saltuk, O., Hang, A., Stolz, K., Bulling, A., and Alt, F. (2016). Textpursuits: Using text for pursuits-based interaction and calibration on public displays. In *Proc. of the 2016 ACM Int. Joint Conf. on Pervasive and Ubiquitous Computing*, UbiComp '16, pages 274–285.

Nagamatsu, T., Kamahara, J., and Tanaka, N. (2009). Calibration-free gaze tracking using a binocular 3d eye model. In *CHI '09 Extended Abstracts on Human Factors in Computing Systems*, pages 3613–3618.

Nishino, K. and Nayar, S. K. (2006). Corneal imaging system: Environment from eyes. *Int. J. Comput. Vision*, 70(1):23–40.

Nitschke, C. and Nakazawa, A. (2012). Super-resolution from corneal images. In *Proc. of the British Machine Vision Conference*, pages 22.1–22.12.

Sugano, Y. and Bulling, A. (2015). Self-calibrating head-mounted eye trackers using egocentric visual saliency. In *Proc. of the 28th Annual ACM Symp. on User Interface Software & Technology*, UIST '15, pages 363–372.

Takemura, K., Yamakawa, T., Takamatsu, J., and Ogasawara, T. (2014). Estimation of a focused object using a corneal surface image for eye-based interaction. *Journal of eye movement research*, 7(3):4:1–9.

Wang, H., Lin, S., Liu, X., and Kang, S. B. (2005). Separating reflections in human iris images for illumination estimation. *IEEE Int. Conf. on Computer Vision*, 2:1691–1698.